Optics Communications 445 (2019) 291–295

Contents lists available at ScienceDirect

Optics Communications

journal homepage: www.elsevier.com/locate/optcom

Optical bistability in a Λ-type atomic system including near dipole–dipole interaction

Juan D. Serna [a], Amitabh Joshi [b,*]

[a] Department of Physics and Electrical Engineering, University of Scranton, Scranton, PA 18510, USA
[b] Department of Physics and Optical Engineering, Rose-Hulman Institute of Technology, Terre Haute, IN 47803, USA

ARTICLE INFO

Keywords:
Optical bistability
Electromagnetically induced transparency
Near dipole–dipole interactions
Three-level atom

ABSTRACT

The advantage of optical bistability (OB) using three-level electromagnetically induced transparency (EIT) atomic system over the two-level system is its controllability, as absorption, dispersion, and optical nonlinearity in one of the atomic transitions can be modified considerably by the field interacting with nearby atomic transition. This is due to induced atomic coherences generated in such EIT system. The inclusion of near dipole–dipole (NDD) interaction among atoms further modifies absorption, dispersion, and optical nonlinearity of three-level EIT system and the OB can also be controlled by this interaction, producing OB to multistability.

1. Introduction

Atomic optical bistability (AOB) is a phenomenon that exploits both the cooperative nature of the interaction between a group of atoms with the field and its strong nonlinearity. The essential element in AOB is the nonlinear relation between the applied electromagnetic field and the electromagnetic field that is radiated by the atomic dipoles, when the actions of all the other dipoles are taken into account. Cooperative radiation therefore plays a key role in bistability [1].

The optical bistability (OB) in an ensemble of two-level atomic systems contained inside an optical cavity has been extensively studied in the decade of eighties and early years of nineties. The studies were focused mainly on to utilize the phenomenon of OB in optical memories, optical transistor-like systems and all-optical switches [2,3]. The observed phenomenon of OB is classified as absorptive OB if the atomic transition is saturated. On the other hand the intensity-dependent refractive index of the media is the mechanism for generating dispersive OB [2–7].

OB is a phenomenon that exploits both the cooperation among atoms and the strong nonlinearity produced by the interacting field. The two-level OB systems show first-order, phase transition-like behavior because in the Fokker–Planck equation the diffusion coefficient is intensity dependent [8,9]. Several interesting theoretical and experimental works reported for the two-level OB systems in the past are well documented in the literature. However, experiments with two-level OB systems have limitations due to the lack of control in generating desirable OB curves with the help of only one field. The electromagnetically induced transparency (EIT) phenomena and related quantities in multi-level systems, such as dispersion and nonlinearity, have given a significant impact on the control of OB and optical multistability in such systems [10–17]. In multi-level systems, the two or more interacting fields generate the induced atomic coherence, which modifies the linear absorption, dispersion and enhances the third-order Kerr nonlinear index of refraction.

Some studies on the behavior of nonlinearity with intensities and frequency detunings of both probe and coupling beams were reported for experiments in the Λ-type atomic system, useful to demonstrate the controllability of OB [18]. Controlling of OB hysteresis cycle is useful in all-optical switches, optical memories, optical transistors, and logic circuits. This control will avoid optical–electronic–optical conversion of information in the form of signals. Atomic coherence in EIT systems enhances Kerr nonlinearity, bringing down the switching thresholds of such devices. Thus the control becomes more accessible and efficient at low-intensity levels of light.

The cavity output field of the atom-field composite system for some parametric conditions becomes unstable, giving rise to dynamic instability and chaos as the optical pumping in the coupling transition competes with the saturation in the probe transition [19,20]. This instability is achieved by adjusting the coupling beam intensity or frequency detuning. The phenomenon of stochastic resonance [21] in optical bistability is also reported in three-level systems. The noise induced switching phenomenon [22,23] in three-level bistable systems is also observed, not available with the two-level systems conveniently.

Propagation of electromagnetic field can generate near dipole–dipole (NDD) interaction in a collection of atoms. The NDD effects can introduce the inversion-dependent-chirping of the atomic resonance frequency in a two-level atomic sample. The microscopic field-atom coupling can be modified due to NDD effect. The microscopic field

* Corresponding author.
E-mail addresses: juan.serna@scranton.edu (J.D. Serna), mcbamji@gmail.com (A. Joshi).

https://doi.org/10.1016/j.optcom.2019.04.045
Received 18 January 2019; Received in revised form 5 April 2019; Accepted 15 April 2019
Available online 18 April 2019

results from the composition of the macroscopic field with the induced polarization [24]. The NDD interaction is realized in a dense medium from entities confined in a tiny volume of the order of a cubic wavelength. The modified Maxwell–Bloch equation in which NDD effects are included gives some extraordinary results such as invariant pulse propagation that departs from the hyperbolic secant pulse shape of self-induced transparency (SIT) [25] and self-phase modulation in SIT [26]. The interaction of the external driving field with an atomic sample generates reaction field that works against the driving field causing reduction of the total field. The effect of a strong external driving field in comparison to the generated reaction field due to the dipole–dipole interaction results in a first-order phase transition far away from the equilibrium due to the suppression of the reaction field [27,28]. The Bose–Einstein condensates can be realized at high temperatures [29] with the help dipole–dipole interaction. In systems used for quantum information processing the entanglement of qubits [30] can be achieved through dipole–dipole interaction. Dipole–Dipole interaction is also crucial during the photosynthesis process [31,32]. The desired value of dipole–dipole or NDD interaction among entities can be achieved by a change of the number density. The dipole–dipole interaction strength and its direction depend on environmental electromagnetic field modes, which can be obtained by directional stop-gaps or manipulating degeneration of the field modes [33,34]. By using specific optical confinement structures, the desired dipole–dipole interaction can be realized [35,36].

Recently, the dynamical evolution of a three-level Λ-type atomic system including near dipole–dipole interaction was investigated. The linear and third order non-linear susceptibilities for the probe transition was studied, and details of absorption and dispersion in the probe transition and dynamic evolution of the system were obtained [37]. This work aims to study the phenomenon of OB in a three-level Λ-type system including NDD interaction among atoms and thus demonstrate the controllability of OB via NDD interaction.

The remaining paper is organized as follows. In Section 2 the model for this work for OB is described. Numerical results for OB are discussed in Section 3 by the solution of the exact density matrix equation. In Section 4 some concluding remarks are presented.

2. The model

We consider a cavity illustrated in Fig. 1, in which there is a nonlinear medium of length L in one arm, driven by a field E_P^I that travels the medium in one direction only [23,38]. We assume that the input and output mirrors, M_1 and M_2, have identical reflectance $\sqrt{R}$ and transmittance $\sqrt{T}$ amplitudes (with $T = 1 - R$), whereas the other two mirrors are fully reflecting ($R = 1$). We also assume that the mirror separation ℓ is adjusted so that the cavity is tuned to near resonance with the applied fields. The nonlinear medium consists of a three-level atomic system with energy levels E_i ($i = 1, 2, 3$) and in a Λ-type configuration ($E_2 > E_3 > E_1$), interacting with probe and coupling lasers of frequencies ω_P and ω_C, with amplitudes E_P and E_C, respectively (see Fig. 2). The probe laser acts on the dipole-allowed transition $|1\rangle \rightarrow |2\rangle$, with energy difference ω_{21} and frequency detuning $\Delta_P = \omega_P - \omega_{21}$. The coupling laser couples to the other dipole-allowed transition $|2\rangle \rightarrow |3\rangle$, with energy difference ω_{23} and frequency detuning $\Delta_C = \omega_C - \omega_{23}$.

In the semiclassical approximation, where the system interacts with the classical electromagnetic fields of the two lasers, the Liouville equations of the density-matrix elements in the dipole and rotating wave approximation, including NDD interaction as described in [37], have the form

$$\dot{\rho}_{22} - \dot{\rho}_{11} = -(\gamma_{23} + 2\gamma_{21})\rho_{22} + 2i\mu_{12}(\varepsilon_L^P)^*\rho_{21} - 2i\mu_{12}(\varepsilon_L^P)\rho_{12} + i\mu_{23}(\varepsilon_L^C)^*\rho_{23} - i\mu_{23}(\varepsilon_L^C)\rho_{32} - \gamma_{31}(\rho_{33} - \rho_{11}) - \gamma_{21}^D|\rho_{21}|^2, \quad (1a)$$

$$\dot{\rho}_{22} - \dot{\rho}_{33} = -(2\gamma_{23} + \gamma_{21})\rho_{22} + i\mu_{12}(\varepsilon_L^P)^*\rho_{21} - i\mu_{12}(\varepsilon_L^P)\rho_{12} + 2i\mu_{23}(\varepsilon_L^C)^*\rho_{23} - 2i\mu_{23}(\varepsilon_L^C)\rho_{32} - \gamma_{31}(\rho_{11} - \rho_{33}) - \gamma_{23}^D|\rho_{23}|^2, \quad (1b)$$

$$\dot{\rho}_{23} = -i[\Delta_C - \epsilon_c(\rho_{22} - \rho_{33})]\rho_{23} - [\gamma - (\gamma_{23}^D/2)(\rho_{22} - \rho_{33})]\rho_{23} + i\mu_{23}(\varepsilon_L^C)(\rho_{22} - \rho_{33}) - i\mu_{12}(\varepsilon_L^P)\rho_{13}, \quad (1c)$$

$$\dot{\rho}_{21} = -i[\Delta_P - \epsilon_p(\rho_{22} - \rho_{11})]\rho_{21} - [\gamma - (\gamma_{21}^D/2)(\rho_{22} - \rho_{11})]\rho_{21} + i\mu_{12}(\varepsilon_L^P)(\rho_{22} - \rho_{11}) - i\mu_{23}(\varepsilon_L^C)\rho_{31}, \quad (1d)$$

$$\dot{\rho}_{31} = -[\gamma_{31} + i(\Delta_P - \Delta_C)]\rho_{31} - i[\epsilon_p(\rho_{22} - \rho_{11}) - \epsilon_c(\rho_{22} - \rho_{33})]\rho_{31} - i\mu_{23}(\varepsilon_L^C)^*\rho_{21} + i\mu_{12}(\varepsilon_L^P)\rho_{32}, \quad (1e)$$

where ε_L^P and ε_L^C are complex, microscopic, slowly-varying electric field envelopes of the probe and coupling fields, respectively; γ_{21} and γ_{23} are the radiative decay rates from level $|2\rangle$ to levels $|1\rangle$ and $|3\rangle$, respectively; population decays from level $|3\rangle$ back to level $|1\rangle$ at a rate γ_{31} in non-radiative manner, and we define $\gamma = \frac{1}{2}(\gamma_{21} + \gamma_{23} + \gamma_{31})$; $\Omega_P = 2\mu_{12}\,\varepsilon_L^P$ is the Rabi frequency of the probe field and ($\Omega_C = 2\mu_{23}\,\varepsilon_L^C$) the Rabi frequency of the coupling field; μ_{12} is the dipole matrix element for transition $|1\rangle \rightarrow |2\rangle$ and μ_{23} for transition $|2\rangle \rightarrow |3\rangle$. Eqs. (1) describe the atomic dynamics of the system.

The imaginary part of the dipole–dipole interaction term for the probe transition is defined as $\epsilon_P = 4i\pi N|\mu_{12}|^2/3\hbar$, and the real part of the dipole–dipole interaction term (dipole–dipole induced decay rate due to NDD interaction from level $|2\rangle$ to level $|1\rangle$) is defined as $\gamma_{21}^D = 2\pi k N|\mu_{12}|^2 d/\hbar$ [37]. Here, d is the thickness of the atomic medium, N is the atomic number density, and k is the wave number for the transition. Likewise, one can define these terms for the coupling transition. Physically, the imaginary part of the dipole–dipole interaction leads to *population difference dependent dynamical shift* in the atomic resonance frequency. On the other hand, the real part leads to *population difference*

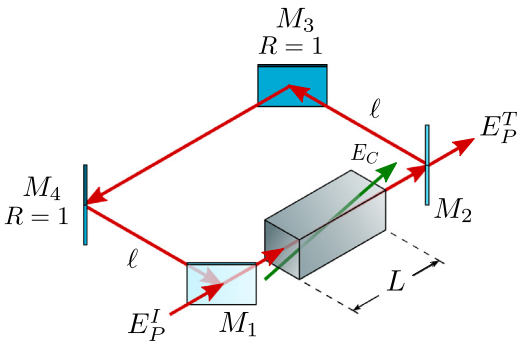

Fig. 1. Schematic diagram of a unidirectional ring cavity having four mirrors (M_1–M_4) and an atomic vapor cell of length L. Mirrors M_3 and M_4 are perfectly reflecting mirrors ($R = 1$). The incident and transmitted fields are represented by E_P^I and E_P^T, respectively, while the coupling field is represented by E_C.

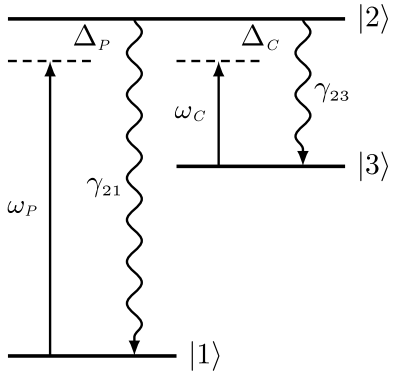

Fig. 2. Schematic diagram of the three-level system in a Λ-configuration driven by probe and coupling lasers of frequencies ω_P and ω_C, respectively.

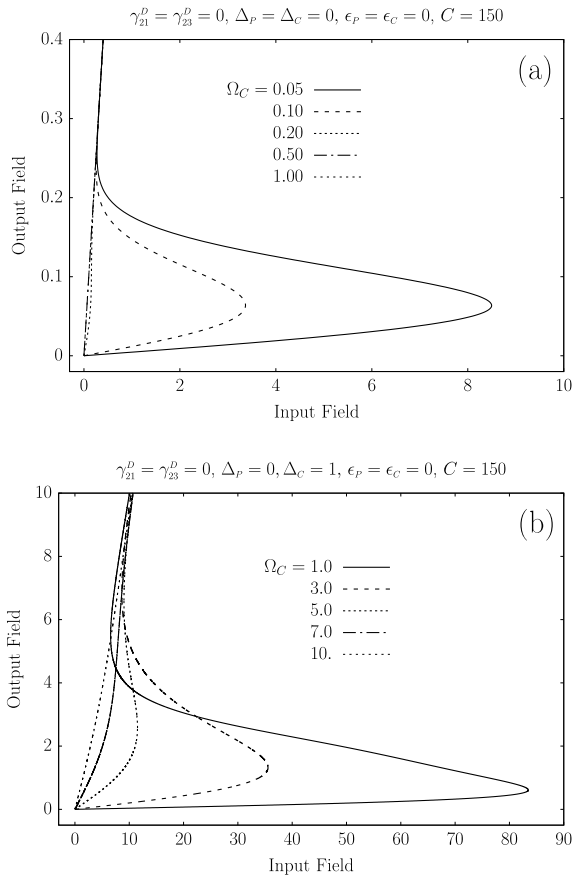

Fig. 3. Optical bistability (in terms of output vs. input cavity field) for a three-level system in Raman configuration of its states. The Rabi frequency Ω_C is variable. (a) $\Delta_C = 0$, (b) $\Delta_C = 1.0$.

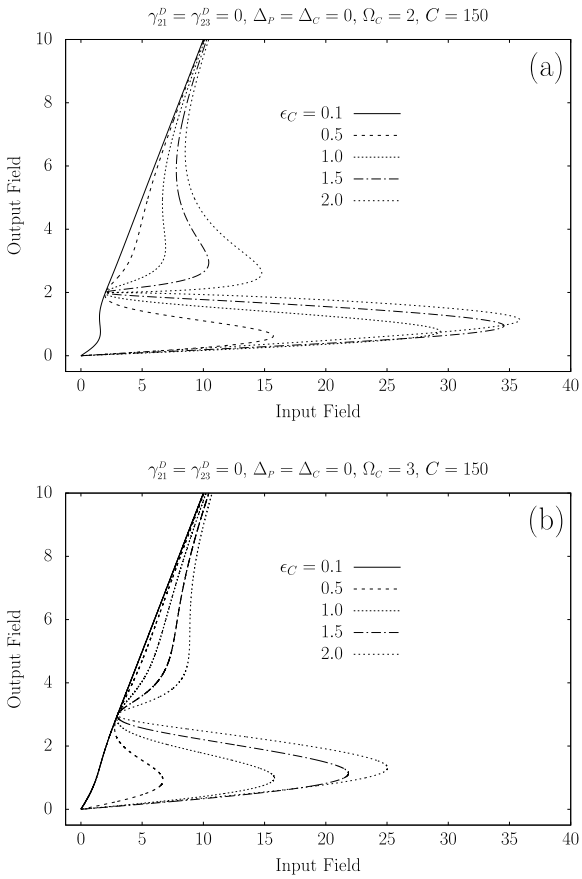

Fig. 4. Output vs. input cavity field of the system as a result of non-zero, near dipole–dipole interaction (NDD). NDD (imaginary part) parameter ϵ_C is variable. (a) $\Omega_C = 2.0$, (b) $\Omega_C = 3.0$.

dependent cooperative relaxation (decay) and the dephasing [24]. The origin of this term is due to the cooperativity of atoms. Thus the population difference dependent cooperative relaxation and dephasing are cooperative in nature, different from the usual radiative decay of population and dephasing.

The combined electric field acting on each atom inside the cavity is the sum of the probe and coupling fields, so that

$$\vec{\mathbf{E}} = (\vec{\mathbf{E}}_P\, e^{-i\omega_P t} + \vec{\mathbf{E}}_C\, e^{-i\omega_C t} + c.c.). \tag{2}$$

The probe field E_P at frequency ω_P (interacting with the atomic transition $|1\rangle \rightarrow |2\rangle$) circulates inside the cavity acting as the cavity field. The coupling field E_C at frequency ω_C (coupling transition $|3\rangle \rightarrow |2\rangle$) does not circulate inside the optical ring cavity as shown in Fig. 1. However, the two fields propagate through the nonlinear medium in the same direction with a very slight angle between the two beams so that the coupling beam does not circulate in the cavity, and the first-order Doppler effect in this three-level, EIT system can be eliminated [16]. The coupling field behaves like a controlling field. The field E_P enters the cavity from the partially transparent mirror M_1 and drives the nonlinear medium. To determine the field inside the unidirectional ring cavity, we write the relations obtained by boundary conditions [38]

$$E_P^T = \sqrt{T}\, E_P(L,t), \tag{3}$$

$$E_P(0,t) = \sqrt{T}\, E_P^I(t) + R\, e^{-i\delta_0}\, E_P(L, t-\Delta t), \tag{4}$$

where the length of the atomic sample is specified by the parameter L, the side arm length between M_2 and M_3 (and also M_4 and M_1) is ℓ, and the time taken by light to travel from mirror M_2 to M_1 via mirrors M_3 and M_4 is given by $\Delta t = (2\ell + L)/c$. The cavity frequency detuning is defined as $\delta_0 = (\omega_{\text{cav}} - \omega_P)L_T/c$, where ω_{cav} is the frequency of the nearest cavity mode to ω_P, and $L_T \approx 2(\ell + L)$ represents the round-trip length of the ring cavity.

The dynamical evolution of the probe field inside the optical cavity is described by the Maxwell's equation (in the slowly-varying envelope approximation) [38]

$$\frac{\partial E_P}{\partial t} + c\frac{\partial E_P}{\partial z} = 2\pi i\, \omega_P \mu_{12} P(\omega_P), \tag{5}$$

where $P(\omega_P) = N\mu_{12}\rho_{12}$ is the induced atomic polarization responsible for AOB, and N is the number density of atoms. In order to obtain the polarization $P(\omega_P)$, one needs to first solve the set of density-matrix equations (1) in the steady-state limit, then integrate (5) over the length of the atomic sample using (3) and (4). The steady-state boundary conditions can be written as [38]

$$E_P^T = \sqrt{T}\, E_P(L), \tag{6}$$

$$E_P(0) = \sqrt{T}\, E_P^I(t) + R\, e^{-i\delta_0}\, E_P(L). \tag{7}$$

3. Results and discussion

We solved Eqs. (1) numerically and plotted the cavity output field (E_P^T) versus the cavity input field (E_P^I) for various parametric values of the coupling field and NDD interaction parameter. We used a semi-implicit extrapolation algorithm from Numerical Recipes (`StepperSie`) [39] as the system of differential equations is stiff. The output–input features for a system showing OB are shown in Fig. 3–6, with all parameters measured in terms of γ (with $\gamma_{31} = 0$ for simplicity). The model here could be experimentally realized in a three-level atomic system consisting of a ^{87}Rb vapor as described in Refs. [23,38,40].

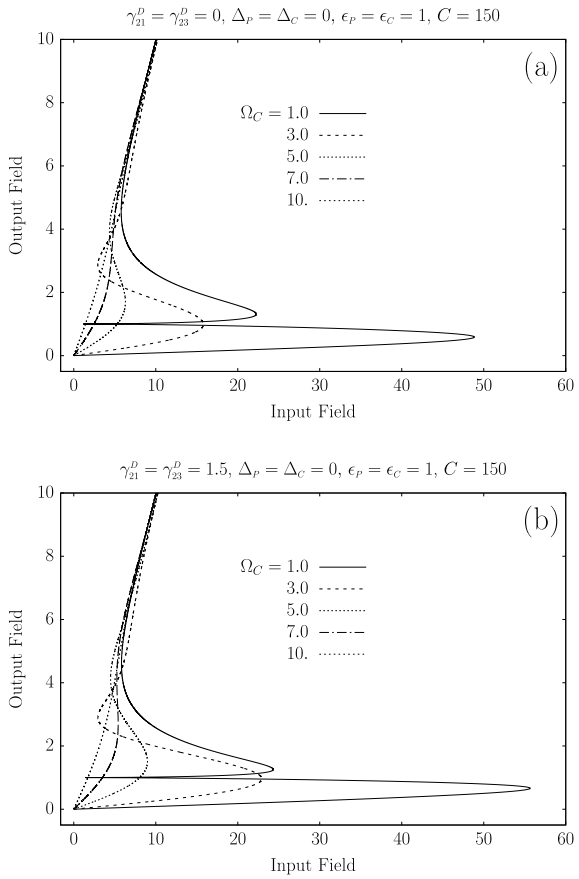

Fig. 5. Output vs. input cavity field of the system for non-zero, near dipole–dipole interaction with $\epsilon_P = \epsilon_C = 2.0$. The Rabi frequency Ω_C is variable. NDD (real part) parameters γ_{21}^D and γ_{23}^D are changed as: (a) $\gamma_{21}^D = \gamma_{23}^D = 0$, (b) $\gamma_{21}^D = \gamma_{23}^D = 1.5$.

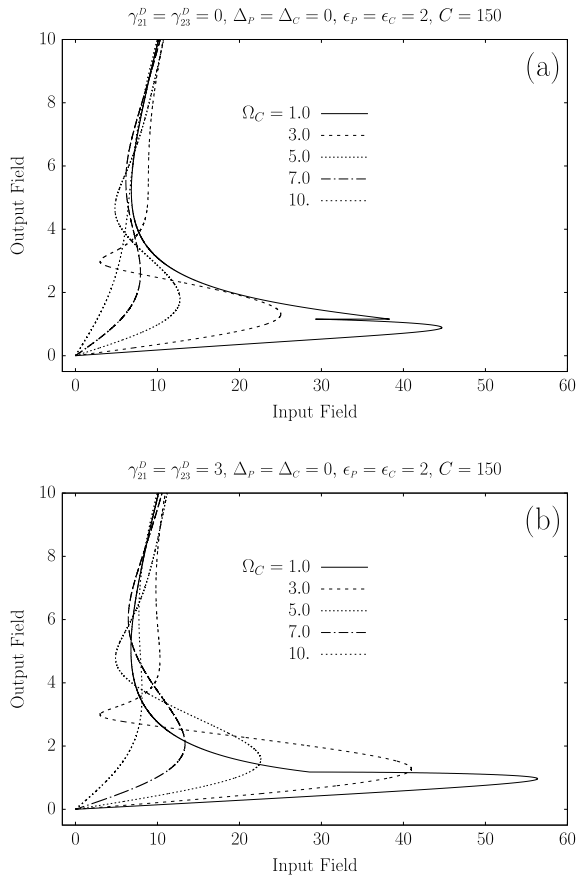

Fig. 6. Same as Fig. 5, with $\epsilon_P = \epsilon_C = 2.0$. (a) $\gamma_{21}^D = \gamma_{23}^D = 0$, (b) $\gamma_{21}^D = \gamma_{23}^D = 3.0$.

The atomic transition frequency is of the order of 10^{15} Hz (wavelength $\sim$ 794.8 nm) with probe transition $(F = 1, 5^2S_{1/2}) \rightarrow (F' = 2, 5^2P_{1/2})$ and coupling transition $(F = 2, 5^2S_{1/2}) \rightarrow (F' = 2, 5^2P_{1/2})$ separated by 6.837 GHz. The typical amplitude of the coupling field in terms of the coupling laser power is 9–10 mW, while the probe beam is varied from zero to 1.5 mW. Finally, $\gamma_{21} = \gamma_{23} \sim 2\pi \times 4.0$ MHz, and $\gamma_{31} = 0$.

Fig. 3(a) shows the curves for a three-level system in Raman configuration of its levels with no dipole–dipole interaction for different Ω_C values of the coupling field. The atomic sample is kept inside the cavity (see Fig. 1). The parameters used were $\gamma_{21}^D = \gamma_{23}^D = 0$, $\Delta_P = \Delta_C = 0$, $\epsilon_P = \epsilon_C = 0$, and $C = 150$ as the cooperative parameter for OB [38]. We changed Ω_C to 0.05, 0.1, 0.2, 0.5, and 1.0. For a small Ω_C, the OB threshold was large (solid line curve). When we increased Ω_C, the threshold decreased, as seen in the figure. For a very large Ω_C, the OB feature disappeared. The effect of a finite detuning of the coupling field is shown in Fig. 3(b). Here, the only parameter modified was $\Delta_C = 1.0$ leaving the other parameters unchanged. The non-zero coupling field detuning enhanced the OB threshold, as it can be observed by comparing the solid lines in Fig. 3(a) and (b). This threshold decreased for bigger values of the coupling field. The different curves correspond to values of $\Omega_C = 1.0$, 3.0, 5.0, 7.0, and 10 (see [38]).

Fig. 4(a) and (b) showed the impact of non-zero, imaginary part of NDD interaction. We used parameters $\gamma_{21}^D = \gamma_{23}^D = 0$, $\Delta_P = \Delta_C = 0$, $\Omega_C = 2.0$, and $C = 150$. The effect of the imaginary part of NDD interaction is depicted in the curves plotted (Fig. 4(a)) for $\epsilon_P = \epsilon_C = 0.1$, 0.5, 1.0, 1.5, and 2.0. For smaller values of ϵ (0.1, 0.5), the curves showed OB. For a further increase in the value of ϵ (1.0, 1.5, 2.0), we observed the interesting phenomenon of optical multistability in the curves. The threshold of all these OB and multistability curves can be altered by modifying the value of the coupling field because this changes the induced coherence and hence the threshold. One such interesting study is shown in Fig. 4(b), where we changed Ω_C to 3.0 but kept all other parameters the same. By doing so, the threshold of OB and multistability curves came down. Again, this was due to the altered induced coherence consistent with the experimental observation of OB [38].

In Fig. 5(a) and (b), we showed the controllability of OB by keeping the values of an NDD interaction parameter fixed. Parameters used for Fig. 5(a) were $\gamma_{21}^D = \gamma_{23}^D = 0$, $\Delta_P = \Delta_C = 0$, $C = 150$, and $\epsilon_C = \epsilon_P = 1.0$. We plotted curves for $\Omega_C = 1.0$, 3.0, 5.0, 7.0 and 10.0. At lower values of Ω_C (1.0 and 3.0), we found multistability that gradually changed to OB as Ω_C further increased to 5.0, 7.0 and 10.0. Thus for a fixed value of the NDD parameter ϵ (imaginary part), the transition from OB to multistability can be controlled by changing the coupling field strength. However, when we introduced the real part of a NDD parameter, such as $\gamma_{21}^D = \gamma_{23}^D = 1.5$ in Fig. 5(b), the shape of all curves remained similar to those in Fig. 5(a) but the OB threshold of all curves increased. This effect is because of the associated increase in the system's dampening that reduces the induced coherence.

For Fig. 6(a), the values for the NDD parameters were $\epsilon_C = \epsilon_P = 2.0$, $\gamma_{21}^D = \gamma_{23}^D = 0.0$, while for Fig. 6(b), the values were $\epsilon_C = \epsilon_P = 2.0$, and $\gamma_{21}^D = \gamma_{23}^D = 3.0$. Fig. 6(a) and (b) showed reduction in the multistability structure for $\Omega_C = 1.0$ when compared with Fig. 5(a) and (b). $\Omega_C = 3.0$ still showed multistability, but the threshold raised as compared to those in Fig. 5(a) and (b). For further increase in Ω_C, all curves displayed OB but with an augmented threshold value. The physical interpretation of these results is implicit in the manipulation of the physical properties of the three-level, EIT medium considered in this work. We achieved this by varying the coupling field and the NDD interaction parameters in the atomic system that changed its generated

atomic coherence [37]. While keeping the coupling field constant, we varied the NDD parameters to control absorption, dispersion, and nonlinearity of the medium and to get changes in its OB.

4. Conclusion

In this work, we studied the optical bistability displayed by a three-level, Λ-type electromagnetic induced transparency medium including near dipole–dipole interaction. The inclusion of NDD interaction provided another control parameter for changing the absorption, dispersion, and nonlinearity of such EIT system. In fact, by modifying the number density of the atomic medium, we may obtain wanted values of NDD parameters. Consequently, by the combined effect of the coupling field and NDD interaction parameters, the system exhibits interesting changes as it passes from OB to optical multistability.

Acknowledgment

We are thankful to G. Duree (RHIT) for his interest and support for this work.

References

[1] L. Mandel, E. Wolf, Optical Coherence and Quantum Optics, Cambridge University Press, New York, 1995.
[2] L.A. Lugiato, Theory of optical bistability, in: E. Wolf (Ed.), Progress in Optics, Vol. 21, North Holland, Amsterdam, 1984, pp. 69–216.
[3] H.M. Gibbs, Optical Bistability: Controlling Light with Light, Academic Press, Orlando, 1985.
[4] H.M. Gibbs, S.L. McCall, T.N.C. Venkatesan, Differential gain and bistability using a sodium-filled fabry-perot interferometer, Phys. Rev. Lett. 36 (1976) 1135–1138, http://dx.doi.org/10.1103/PhysRevLett.36.1135.
[5] T.N.C. Venkatesan, S.L. McCall, Optical bistability and differential gain between 85 and 296∘k in a fabry-perot containing ruby, Appl. Phys. Lett. 30 (1977) 282–284, http://dx.doi.org/10.1063/1.89368.
[6] G.P. Agrawal, H.J. Carmichael, Optical bistability through nonlinear dispersion and absorption, Phys. Rev. A 19 (1979) 2074–2086, http://dx.doi.org/10.1103/PhysRevA.19.2074.
[7] R.B. Boyd, Nonlinear Optics, third ed., Academic Press, Boston, 2008.
[8] L.A. Lugiato, J.D. Farina, L.M. Narducci, Quantum-statistical treatment of the transient in absorptive optical bistability—local relaxation, Phys. Rev. A 22 (1980) 253–260, http://dx.doi.org/10.1103/PhysRevA.22.253.
[9] L.A. Lugiato, V. Benza, L.M. Narducci, J.D. Farina, Optical bistability, instabilities and higher order bifurcations, Opt. Commun. 39 (1981) 405–410, http://dx.doi.org/10.1016/0030-4018(81)90233-9.
[10] E. Arimondo, Coherent population trapping in laser spectroscopy, in: E. Wolf (Ed.), Progress in Optics, Vol. 35, North Holland, Amsterdam, 1996, pp. 257–354.
[11] S.E. Harris, Electromagnetically induced transparency, Phys. Today 50 (1997) 36–42, http://dx.doi.org/10.1063/1.881806.
[12] J.P. Marangos, Electromagnetically induced transparency, J. Modern Opt. 45 (1998) 471–503, http://dx.doi.org/10.1080/09500349808231909.
[13] K.J. Boller, A. Imamoğ, S.E. Harris, Observation of electromagnetically induced transparency, Phys. Rev. Lett. 66 (1991) 2593–2596, http://dx.doi.org/10.1103/PhysRevLett.66.2593.
[14] J.E. Field, K.H. Hahn, S.E. Harris, Observation of electromagnetically induced transparency in collisionally broadened lead vapor, Phys. Rev. Lett. 67 (1991) 3062–3065, http://dx.doi.org/10.1103/PhysRevLett.67.3062.
[15] Y.-q. Li, M. Xiao, Electromagnetically induced transparency in a three-level Λ-type system in rubidium atoms, Phys. Rev. A 51 (1995) R2703–R2706, http://dx.doi.org/10.1103/PhysRevA.51.R2703.
[16] J. Gea-Banacloche, Y.-q. Li, S.-z. Jin, M. Xiao, Electromagnetically induced transparency in ladder-type inhomogeneously broadened media: Theory and experiment, Phys. Rev. A 51 (1995) 576–584, http://dx.doi.org/10.1103/PhysRevA.51.576.
[17] M. Xiao, Y.-q. Li, S.-z. Jin, J. Gea-Banacloche, Measurement of dispersive properties of electromagnetically induced transparency in rubidium atoms, Phys. Rev. Lett. 74 (1995) 666–669, http://dx.doi.org/10.1103/PhysRevLett.74.666.
[18] H. Wang, D. Goorskey, M. Xiao, Enhanced Kerr nonlinearity via atomic coherence in a three-level atomic system, Phys. Rev. Lett. 87 (2001) 073601, http://dx.doi.org/10.1103/PhysRevLett.87.073601.
[19] W. Yang, A. Joshi, M. Xiao, Controlling dynamic instability of three-level atoms inside an optical ring cavity, Phys. Rev. A 70 (2004) 033807, http://dx.doi.org/10.1103/PhysRevA.70.033807.
[20] W. Yang, A. Joshi, M. Xiao, Chaos in an electromagnetically induced transparent medium inside an optical cavity, Phys. Rev. Lett. 95 (2005) 093902, http://dx.doi.org/10.1103/PhysRevLett.95.093902.
[21] A. Joshi, M. Xiao, Stochastic resonance in atomic optical bistability, Phys. Rev. A 74 (2006) 013817, http://dx.doi.org/10.1103/PhysRevA.74.013817.
[22] A. Joshi, M. Xiao, Noise-induced switching via fluctuating atomic coherence in an optical three-level bistable system, J. Opt. Soc. Amer. B 25 (2008) 2015–2020, http://dx.doi.org/10.1364/JOSAB.25.002015.
[23] A. Joshi, M. Xiao, Controlling nonlinear optical processes in multi-level atomic systems, in: E. Wolf (Ed.), Progress in Optics, Vol. 49, North Holland, Amsterdam, 2006, pp. 97–175.
[24] C.M. Bowden, Near dipole–dipole interaction effects in quantum and nonlinear optics, in: I. Ramarao (Ed.), Recent Developments in Quantum Optics, Plenum Press, New York, 1993, pp. 55–63.
[25] C.M. Bowden, A. Postan, R. Inguva, Invariant pulse propagation and self-phase modulation in dense media, J. Opt. Soc. Amer. B 8 (1991) 1081–1084, http://dx.doi.org/10.1364/JOSAB.8.001081.
[26] C. Stroud, C. Bowden, L. Allen, Self-induced transparency in self-chirped media, Opt. Commun. 67 (1988) 387–390, http://dx.doi.org/10.1016/0030-4018(88)90033-8.
[27] R. Inguva, C.M. Bowden, Spatial and temporal evolution of the first-order phase transition in intrinsic optical bistability, Phys. Rev. A 41 (1990) 1670–1676, http://dx.doi.org/10.1103/PhysRevA.41.1670.
[28] Y. Ben-Aryeh, C. Bowden, J. Englund, Longitudinal spacial first-order phase transition in a system of coherently-driven, two-level atoms, Opt. Commun. 61 (1987) 147–150, http://dx.doi.org/10.1016/0030-4018(87)90237-9.
[29] S. Yang, S. John, Exciton dressing and capture by a photonic band edge, Phys. Rev. B 75 (2007) 235332, http://dx.doi.org/10.1103/PhysRevB.75.235332.
[30] G.K. Brennen, I.H. Deutsch, P.S. Jessen, Entangling dipole–dipole interactions for quantum logic with neutral atoms, Phys. Rev. A 61 (2000) 062309, http://dx.doi.org/10.1103/PhysRevA.61.062309.
[31] R. El-Ganainy, S. John, Resonant dipole–dipole interaction in confined and strong-coupling dielectric geometries, New J. Phys. 15 (2013) 083033, http://dx.doi.org/10.1088/1367-2630/15/8/083033.
[32] M. Mohseni, P. Rebentrost, S. Lloyd, A. Aspuru-Guzik, Environment-assisted quantum walks in photosynthetic energy transfer, J. Chem. Phys. 129 (2008) 174106, http://dx.doi.org/10.1063/1.3002335.
[33] T. Kobayashi, Q. Zheng, T. Sekiguchi, Resonant dipole–dipole interaction in a cavity, Phys. Rev. A 52 (1995) 2835–2846, http://dx.doi.org/10.1103/PhysRevA.52.2835.
[34] G.S. Agarwal, S.D. Gupta, Microcavity-induced modification of the dipole–dipole interaction, Phys. Rev. A 57 (1998) 667–670, http://dx.doi.org/10.1103/PhysRevA.57.667.
[35] M. Hopmeier, W. Guss, M. Deussen, E.O. Göbel, R.F. Mahrt, Enhanced dipole–dipole interaction in a polymer microcavity, Phys. Rev. Lett. 82 (1999) 4118–4121, http://dx.doi.org/10.1103/PhysRevLett.82.4118.
[36] M.J. Levene, J. Korlach, S.W. Turner, M. Foquet, H.G. Craighead, W.W. Webb, Zero-mode waveguides for single-molecule analysis at high concentrations, Science 299 (2003) 682–686, http://dx.doi.org/10.1126/science.1079700.
[37] A. Joshi, J.D. Serna, Absorption–dispersion in a three-level electromagnetically induced transparency medium including near dipole–dipole interaction effects, Opt. Commun. 430 (2019) 119–130, http://dx.doi.org/10.1016/j.optcom.2018.08.018.
[38] A. Joshi, M. Xiao, Atomic optical bistability in two- and three-level systems: perspectives and prospects, J. Modern Opt. 57 (2010) 1196–1220, http://dx.doi.org/10.1080/09500340.2010.492919.
[39] W.H. Press, S.A. Teukolsky, W.T. Vetterling, B.P. Flannery, Numerical Recipes 3rd Edition: The Art of Scientific Computing, third ed., Cambridge University Press, New York, NY, USA, 2007.
[40] D. Goorskey, H. Wang, W. Burkett, M. Xiao, Effects of a highly dispersive atomic medium inside an optical ring cavity, J. Modern Opt. 49 (2002) 305–317, http://dx.doi.org/10.1080/09500340110089947.